The Journal of Chemical Physics

Influence of spontaneous curvature on the line tension of phase-coexisting domains in a lipid monolayer: A Landau-Ginzburg model

Cite as: J. Chem. Phys. **152**, 054707 (2020); https://doi.org/10.1063/1.5138192
Submitted: 13 November 2019 . Accepted: 12 January 2020 . Published Online: 03 February 2020

Elena Rufeil Fiori, Rachel Downing, Guilherme Volpe Bossa, and Sylvio May

The Journal of Chemical Physics ARTICLE scitation.org/journal/jcp

Influence of spontaneous curvature on the line tension of phase-coexisting domains in a lipid monolayer: A Landau-Ginzburg model

Cite as: J. Chem. Phys. 152, 054707 (2020); doi: 10.1063/1.5138192
Submitted: 13 November 2019 • Accepted: 12 January 2020 •
Published Online: 3 February 2020

Elena Rufeil Fiori,[1] Rachel Downing,[2] Guilherme Volpe Bossa,[3] and Sylvio May[2,a)]

AFFILIATIONS

[1] Facultad de Matemática, Astronomía, Física y Computación and Instituto de Física Enrique Gaviola (IFEG), CONICET, Universidad Nacional de Córdoba, X5000HUA Córdoba, Argentina

[2] Department of Physics, North Dakota State University, Fargo, North Dakota 58108, USA

[3] Department of Physics, São Paulo State University (UNESP), Institute of Biosciences, Humanities and Exact Sciences, São José do Rio Preto, SP 15054-000, Brazil

[a)] **Author to whom correspondence should be addressed:** sylvio.may@ndsu.edu

ABSTRACT

The line tension between two coexisting phases of a binary lipid monolayer in its fluid state has contributions not only from the chemical mismatch energy between the two different lipid types but also from the elastic deformation of the lipid tails. We investigate to what extent differences in the spontaneous curvature of the two lipids affect the line tension. To this end, we supplement the standard Landau-Ginzburg model for the line tension between coexisting phases by an elastic energy that accounts for lipid splay and tilt. The spontaneous curvature of the two lipids enters into our model through the splay deformation energy. We calculate the structure of the interfacial region and the line tension between the coexisting domains numerically and analytically, the former based on the full non-linear model and the latter upon employing an approximation in the free energy that linearizes the resulting Euler-Lagrange equations. We demonstrate that our analytical approximation is in excellent agreement with the full non-linear model and use it to identify relevant length scales and two physical regimes of the interfacial profile, double-exponential decay, and damped oscillations. The dependence of the line tension on the spontaneous curvatures of the individual lipids is crucially dependent on how the bulk phases are affected. In the special case that the bulk phases remain inert, the line tension decreases when the difference between the spontaneous curvatures of the two lipid types grows.

I. INTRODUCTION

Coexisting phases in a lipid monolayer are separated by a thin interfacial region—a domain boundary—that gives rise to a line tension σ. The line tension of two-dimensional domains is the analog of the surface tension in three dimensions.[1] The presence of phase coexistence occurs in a wide variety of lipid monolayers. Depending on the lateral pressure applied to a one-component monolayer at the air-water interface, a sequence of phase transitions may be initiated, including that from the liquid-expanded to the liquid-condensed phase. For a two-component lipid monolayer, composed of a lipid type A and a lipid type B, such a phase separation can also be triggered at a constant applied pressure as a function of the lipid composition (that is, the mole fraction of lipid A). For example, adding the cholesterol analog dihydrocholesterol (dchol) to a lipid monolayer composed of various saturated[2,3] or unsaturated[4] lipids can trigger domain formation. Other mixtures of lipids, such as dipalmitoylphosphatidylcholine (DPPC) and dipalmitoylphosphoglycerol (DPPG), also give rise to the formation of distinct immiscible fluid-like phases.[5] In the heterogeneous environments of mixed monolayers and bilayers, line tension plays an important role for the shapes and sizes of the lipid domains,[1,6] the nucleation kinetics,[7,8] the capture zone of each domain,[9] and the formation and stability of lipid rafts.[10–12]

The line tension σ corresponding to the domain boundary of a lipid monolayer at the air-water interface has been determined based on a variety of methods,[3] including shape relaxation of domains,[2,13] boundary fluctuations,[14–16] and analysis of domain size distributions.[12,17] Using a domain shape relaxation method that employs non-homogeneous electrostatic fields, Bischof *et al.*[2] have found a correlation between line tension σ and spontaneous curvature c_0 of the involved lipids. For binary dchol-phospholipid mixtures, they observed larger σ for phospholipids with a large negative c_0 (such as phosphatidylethanolamine) and smaller σ for lipids with small or vanishing c_0. We have taken this experimental finding as motivation to develop a systematic model that relates the line tension σ to the spontaneous curvatures c_0^A and c_0^B of the two involved lipid types.

Our goal in the present work is to develop and analyze a theoretical formalism to include elastic deformations of a binary lipid monolayer into the calculation of the line tension between two fluid-like coexisting phases based on Landau-Ginzburg theory. Landau-Ginzburg theory has been used in a plethora of studies to describe the structure and phase behavior of lipid membranes,[18,19] vesicles,[20–22] and simple and complex fluids.[23–28] In the absence of an elastic contribution to the monolayer free energy, our model reduces to the well-known mean-field description of the interfacial structure (following a hyperbolic tangent-like profile for an appropriately defined compositional order parameter) and corresponding line tension.[29–31] We take this as a reference with respect to which we analyze the influence of elastic deformations of the lipid monolayer, which we characterize by a second order parameter, the local average tilt angle of the lipid tails with respect to the monolayer normal. While changes in the lipid tilt angle and lipid splay enter into the elastic free energy, we focus on the dependence of the line tension on the spontaneous curvature of the lipids (which contribute to the splay energy). We derive an approximate (and yet very accurate) analytic expression for the line tension and analyze its dependence on the lipid spontaneous curvature for the two physically most interesting cases.

II. THEORY

Consider a lipid monolayer in its fluid state at the air-water interface. The monolayer consists of two lipid types, referred to as "A" and "B," with sufficiently strong mutual repulsion so that it separates into two distinct phases, one rich in A and the other rich in B. The two phases are separated by an interfacial region (a domain boundary) that is associated with a line tension σ, the excess energy per unit length. Our goal is to develop a theoretical model for the line tension, thereby accounting both for the repulsion between lipid A and lipid B that produces the phase separation and for the elastic energy of the lipid monolayer. Separating the "chemical" from the "elastic" interactions allows us to investigate the role that the lipid shape, embodied by the spontaneous curvature of each lipid type, plays for σ.

We describe the monolayer properties locally using two order parameters, the local composition η, defined as the mole fraction of lipid A (ranging from $\eta = 0$ to $\eta = 1$), and the lipid tilt angle θ with respect to the normal direction of the air-water interface. Note that the tilt direction θ reflects an average tilt angle, which even for lipids in their fluid state is a well defined quantity.[32] We place the x-axis of

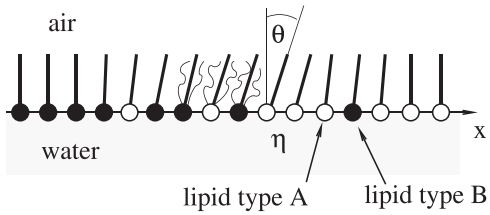

FIG. 1. Schematic illustration of a binary lipid monolayer at the air-water interface that forms two distinct fluid-like bulk phases at $x \to \pm\infty$. The state of the monolayer is fully characterized by the local composition $\eta(x)$ and lipid tilt angle $\theta(x)$, both measured along the x-direction normal to the domain boundary. The lipid director that defines the tilt angle θ represents an average quantity of the lipid tails. The two fluid-like hydrocarbon tails of three lipids are shown schematically.

a Cartesian coordinate system along the air-water interface, which we assume to be straight, normal to the domain boundary. All properties of the monolayer then depend only on x, implying that the two functions $\eta(x)$ and $\theta(x)$ fully characterize the state of the monolayer. Figure 1 illustrates a cross-section of the monolayer along the x-axis schematically.

The free energy $F = F_c + F_e$ of the phase-separated monolayer can be expressed by a "chemical" (index "c") and an "elastic" (index "e") contribution. For the two individual contributions, measured per unit length L of the domain boundary, we write

$$\frac{F_c}{L} = \frac{1}{a}\int_{-\infty}^{\infty} dx\left[f_{BW}(\eta) + \frac{K}{2}\eta'^2\right],$$
$$\frac{F_e}{L} = \int_{-\infty}^{\infty} dx\left[\frac{\kappa_t}{2}\theta^2 + \frac{\kappa}{2}(\theta' - c_0)^2\right], \tag{1}$$

where we express all energies in units of the thermal energy unit k_BT, the Boltzmann constant k_B times the absolute temperature T. Both integrals in Eq. (1) run from $-\infty$ to ∞, where the two distinct phases exist in their bulk state.

The "chemical" contribution [F_c in Eq. (1)] integrates over a local free energy

$$f_{BW}(\eta) = \eta\ln\eta + (1-\eta)\ln(1-\eta) + \chi\eta(1-\eta) \tag{2}$$

and a gradient term (the prime denotes the derivative with respect to x) with a corresponding modulus K. The function $f_{BW}(\eta)$ expresses the mean-field free energy of a binary two-dimensional lattice gas, measured per lattice site. The parameter χ embodies the lipid-lipid interaction strength. Positive χ signifies effective repulsion between lipids of types A and B; in the absence of additional interactions, phase separation takes place for $\chi > 2$. Note that the mean-field approximation of a lattice gas is also known as random mixing approximation, and the corresponding free energy as Bragg-Williams free energy[29] (hence the subscript "BW"). Each site of the lattice gas has a cross-sectional area a, which we identify with the cross-sectional area per lipid. We assume a is constant and uniform for all lipids of the monolayer irrespective of the location and deformation state.

The "elastic" contribution [F_e in Eq. (1)] accounts for the energies associated with lipid tilt, θ, measured relative to the normal

direction of the air-water interface, and lipid splay, θ' (recall that the prime denotes the derivative with respect to x). Three material parameters are contained in F_e: the tilt modulus κ_t, the bending stiffness κ, and the spontaneous curvature c_0. The latter reflects the preferred shape of the lipids, ranging from $c_0 > 0$ for cone-like lipids to $c_0 < 0$ for inverted cone-like lipids. Although the lipid monolayer lays flat on the air-water interface, the lipids are able to undergo a splay deformation by changing the angle θ as function of x. The corresponding modulus κ can be identified as a bending stiffness.[33–35]

The material parameters κ, κ_t, and c_0 contained in F_e may all be functions of the local lipid composition η. While these dependencies will only moderately affect the magnitudes of κ and κ_t, mixing cone-like with inverted cone-like lipids will obviously alter not only the magnitude but also the sign of the spontaneous curvature c_0. In order to most clearly establish the role of the spontaneous curvature, we assume that κ and κ_t are independent of η and that the spontaneous curvature depends linearly on the composition through

$$c_0(\eta) = c_0^A \eta + c_0^B (1-\eta), \tag{3}$$

where c_0^A and c_0^B are the spontaneous curvatures of lipid monolayers consisting only of lipid types A and B, respectively. A lipid monolayer with a free energy F according to Eq. (1) and a spontaneous curvature according to Eq. (3) gives rise to a critical point $\eta = \eta_c$, $\theta = \theta_c$, and $\chi = \chi_c$ with

$$\eta_c = 1/2, \qquad \theta_c = 0, \qquad \chi_c = 2 + \frac{a}{2}\kappa\,(c_0^A - c_0^B)^2. \tag{4}$$

Note that the increase of χ_c beyond 2 can be interpreted in terms of the "frustration energy" that is stored in a planar lipid layer with a composition-dependent spontaneous curvature $c_0(\eta)$. Equation (4) suggests the introduction of the new compositional variable ϕ and the excess lipid-lipid interaction strength $\Delta\chi$ (in excess to the critical value, with $\Delta\chi > 0$) via

$$\eta = \eta_c + \phi, \qquad \chi = \chi_c + \Delta\chi \tag{5}$$

and to expand F in the vicinity of the critical point up to fourth order in ϕ. This yields a Landau-Ginzburg type free energy in terms of the two order parameters $\phi(x)$ and $\theta(x)$,

$$\frac{F}{L} = \frac{1}{a}\int_{-\infty}^{\infty} dx \left\{ -\Delta\chi\,\phi^2 + \frac{4}{3}\phi^4 + a\kappa\bar{c}_0\,\Delta c_0\phi + \frac{K}{2}\phi'^2 + a\left[\frac{\kappa_t}{2}\theta^2 + \frac{\kappa}{2}\theta'^2 - \kappa\theta'(\bar{c}_0 + \Delta c_0\,\phi)\right]\right\}, \tag{6}$$

where we have defined the average, $\bar{c}_0$, and difference, Δc_0, of the spontaneous curvatures of the single-component A and B lipid monolayers via

$$\bar{c}_0 = \frac{c_0^A + c_0^B}{2}, \qquad \Delta c_0 = c_0^A - c_0^B. \tag{7}$$

With these definitions, Eq. (3) now reads $c_0(\phi) = \bar{c}_0 + \Delta c_0\,\phi$. We reiterate that F in Eq. (6) coincides (up to an arbitrary constant) with the free energy $F = F_c + F_e$ in Eq. (1) only in the vicinity of the critical point.

In thermal equilibrium, all lipids of type A must have the same chemical potential μ_A everywhere in the lipid monolayer. An equivalent statement also applies to the chemical potential μ_B of the type-B lipids. Because our model involves only one single compositional degree of freedom (ϕ), the only relevant chemical potential is the difference $\Delta\mu = \mu_A - \mu_B$. We fix $\Delta\mu$ by the Legendre transformation $\tilde{F} = F - (L/a)\int_{-\infty}^{\infty} dx\,\Delta\mu\,\phi$. Minimizing $\tilde{F}$ in the bulk of each coexisting phase (at $x \to \pm\infty$) and accounting for the common-tangent condition of two coexisting phases[29] yields the bulk equilibrium values $\phi(x \to \pm\infty) = \pm\phi_{eq}$ and $\theta(x \to \pm\infty) = \pm\theta_{eq}$ as well as the chemical potential difference $\Delta\mu$. We find

$$\phi_{eq} = \sqrt{\frac{3}{8}\Delta\chi}, \qquad \theta_{eq} = 0, \qquad \Delta\mu = a\kappa\bar{c}_0\,\Delta c_0. \tag{8}$$

The expression for $\Delta\mu$ eliminates the term linear in ϕ from the free energy $\tilde{F}$. This implies [see below in Eqs. (11) and (13)] that the line tension σ does not depend on the average spontaneous curvature $\bar{c}_0$, defined in Eq. (7). That is, it only depends on the difference $\Delta c_0 = c_0^A - c_0^B$, but not on c_0^A and c_0^B individually.

In the following, it is convenient to define the four quantities

$$y(x) = \frac{\phi(x)}{\phi_{eq}}, \quad \xi = \sqrt{\frac{K}{\Delta\chi}}, \quad \tau = \sqrt{\frac{\kappa}{\kappa_t}}, \quad \tilde{a} = \frac{3a\kappa}{16\phi_{eq}^3}. \tag{9}$$

The first one defines the scaled compositional order parameter $y(x)$, which we use instead of $\phi(x)$. The next two define the two characteristic lengths ξ and τ. The final definition, that for $\tilde{a}$, can be viewed as a scaled cross-sectional area per lipid. Using Eqs. (8) and (9), we can express the free energy as

$$\frac{\tilde{F}}{L} = \kappa\int_{-\infty}^{\infty} dx \left\{\phi_{eq}\left[\frac{-y^2 + \frac{1}{2}y^4 + \frac{\xi^2}{2}y'^2}{2\tilde{a}} - \Delta c_0\,\theta' y\right] + \frac{1}{2\tau^2}\theta^2 + \frac{1}{2}\theta'^2\right\}. \tag{10}$$

Thermal equilibrium corresponds to the state of the lowest free energy $\tilde{F}$. To find that state, the functions $y(x)$ and $\theta(x)$ must satisfy the two Euler-Lagrange equations

$$\begin{aligned} \frac{\xi^2}{2}y'' &= -y + y^3 - \tilde{a}\,\Delta c_0\,\theta', \\ \theta'' &= \frac{1}{\tau^2}\theta + \Delta c_0\,\phi_{eq} y', \end{aligned} \tag{11}$$

subject to the four boundary conditions $y(x \to \pm\infty) = \pm 1$ and $\theta(x \to \pm\infty) = 0$. Note that our assumption of a vanishing tilt angle in each bulk phase is justified for lipid monolayers in their fluid state. The two Euler-Lagrange equations and corresponding boundary conditions predict that $y(x) = -y(-x)$ and $\theta(x) = \theta(-x)$ are odd and even functions, respectively.[36] Hence, $y(0) = \theta'(0) = 0$. Using the two Euler-Lagrange equations and corresponding boundary conditions allows us to re-express $\tilde{F}/L$ in Eq. (10) as (see the Appendix for details)

$$\frac{\tilde{F}}{L} = -\frac{4}{3}\frac{\phi_{eq}^4}{a}\int_{-\infty}^{\infty} dx\, y^4. \tag{12}$$

The line tension σ corresponds to the excess free energy with respect to the bulk, where $y(x \to \pm\infty) = \pm 1$. Because $y(x)$ is an odd function,

we can calculate the line tension from

$$\sigma = -\frac{8}{3}\frac{\phi_{eq}^4}{a}\int_0^\infty dx\,\left(y^4-1\right). \tag{13}$$

In summary, to calculate the line tension σ, it is sufficient to integrate the fourth power of the solution $y(x)$ of the Euler-Lagrange equations minus one, from the center of the interface ($x = 0$) into one of the two bulk phases ($x \to \infty$). However, one of the two Euler-Lagrange equations is non-linear, making it non-trivial to find an explicit solution for $y(x)$ and thus an analytic expression for σ. Indeed, we have not succeeded in doing so. Instead, in Sec. III, we will demonstrate excellent agreement between numerical solutions of the present non-linear problem [Eqs. (11) and (13)] and a linearized approximate approach that yields explicit analytic expressions for $y(x)$, $\theta(x)$, and σ.

If lipid types A and B have the same intrinsic spontaneous curvature, then $\Delta c_0 = c_0^A - c_0^B$ vanishes. In this case, the Euler-Lagrange Eq. (11) decouple and give rise to the simple solution

$$y(x) = \tanh\frac{x}{\xi}, \qquad \theta(x) = 0. \tag{14}$$

The compositional order parameter following the function of a hyperbolic tangent across a domain boundary constitutes the well-known[29–31] solution of the phenomenological Landau-Ginzburg approach for simple fluids. Equation (13) then predicts the corresponding line tension

$$\sigma = \frac{32}{9}\frac{\xi}{a}\phi_{eq}^4, \tag{15}$$

which will serve us below as reference for $\Delta c_0 = 0$. That is, we describe the influence of non-vanishing $|\Delta c_0|$ on the line tension relative to Eq. (15). We note that the line tension in Eq. (15) can also be calculated using the relation[29–31]

$$\sigma = \frac{8}{3a}\phi_{eq}^4\xi^2\int_{-\infty}^{\infty} dx\,y'^2, \tag{16}$$

which follows from inserting the first integral $\xi^2 y'^2 = -2y^2 + y^4 + 1$ of the Euler-Lagrange equation $\xi^2 y''/2 = -y + y^3$, subject to $y(x \to \infty) = 1$, into the free energy $\tilde{F}/L$. Indeed, inserting $y(x) = \tanh(x/\xi)$ into Eq. (16) recovers the line tension in Eq. (15). We emphasize that the validity of Eq. (16) is limited to the case $\Delta c_0 = 0$. In contrast, Eq. (13) applies to any choice of Δc_0.

III. RESULTS AND DISCUSSION

We first derive approximate—yet, as we shall demonstrate below, very accurate—analytic expressions for $y(x)$, $\theta(x)$, and σ. We then define a proper reference state and, finally, compare our analytic approximation with numerical solutions of the non-linear formalism developed in Sec. II.

A. Analytic approximation

In order to find approximate expressions for $y(x)$ and $\theta(x)$ as well as for the line tension σ, we employ the symmetries $y(x) = -y(-x)$ and $\theta(x) = \theta(-x)$ to re-express the free energy in Eq. (10) as an integral over the positive region of the x-axis,

$$\frac{\tilde{F}}{L} = 2\kappa\int_0^\infty dx\left\{\phi_{eq}\left[\frac{-y^2+\frac{1}{2}y^4+\frac{\xi^2}{2}y'^2}{2\tilde{a}} - \Delta c_0\,\theta' y\right] + \frac{1}{2\tau^2}\theta^2 + \frac{1}{2}\theta'^2\right\}. \tag{17}$$

Our inability to identify an analytic expression for the free energy minimum of $\tilde{F}/L$ originates in the presence of the fourth-order polynomial $-y^2 + y^4/2$ in the integrand of Eq. (17). Motivated by the work of Gompper and Zschocke,[24] we replace the fourth-order polynomial by two second-order polynomials, one for $y < 0$ and another one for $y > 0$. This double-parabola approximation[37,38] leads to piecewise linear Euler-Lagrange equations that can be solved analytically and may thus give rise to a reasonably simple analytic expression for $\tilde{F}/L$. To ensure a stable bulk phase, the quadratic polynomial should have a local minimum at $y = 1$. We therefore make the ansatz to replace

$$-y^2 + \frac{1}{2}y^4 \to \frac{c^2}{2}(y-1)^2 - \frac{1}{2} \tag{18}$$

in Eq. (17), with a yet to be determined parameter c. Figure 2 shows the function $-y^2 + y^4/2$ (black solid line) together with its approximation $[c^2(y-1)^2 - 1]/2$ for $c = 1$ (blue dashed line), $c = 4/3$ (red dashed line), and $c = 2$ (green dashed line). Clearly, the choice $c = 1$ leads to a match at positions $y = 0$ and $y = 1$. On the other hand, the choice $c = 2$ provides the best fit in the vicinity of $y = 1$.

We determine the value of c such that we reproduce our reference result for σ in Eq. (15) when Δc_0 vanishes. The choice $\Delta c_0 = 0$ leads to $\theta(x) = 0$ and thus leaves us with the free energy

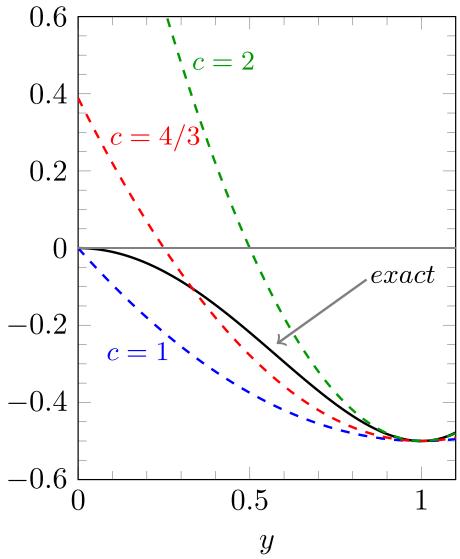

FIG. 2. The function $-y^2 + y^4/2$ (black solid line) together with its approximation $[c^2(y-1)^2 - 1]/2$ (dashed lines), displayed for $c = 1$ (blue), $c = 4/3$ (red), and $c = 2$ (green).

$$\frac{\tilde{F}}{L} = \frac{16}{3}\frac{\phi_{eq}^4}{a}\int_0^\infty dx\left[\frac{c^2}{2}(y-1)^2 - \frac{1}{2} + \frac{\xi^2}{2}y'^2\right], \tag{19}$$

which, subject to $y(0) = 0$ and $y(x \to \infty) = 1$, is minimized by $y(x) = 1 - e^{-cx/\xi}$. This leads to the line tension

$$\sigma = \frac{8}{3}\frac{\xi^2}{a}\phi_{eq}^4 y'(0) = \frac{8}{3}\frac{\xi}{a}\phi_{eq}^4 c. \tag{20}$$

Matching of σ in Eqs. (15) and (20) yields $c = 4/3$. The corresponding approximation is displayed by the red dashed line in Fig. 2. We will use the value $c = 4/3$ in the remainder of the present work.

Based on the approximation introduced in Eq. (18), together with $c = 4/3$, the free energy in Eq. (17) now reads

$$\frac{\tilde{F}}{L} = 2\kappa\int_0^\infty dx\left\{\phi_{eq}\left[\frac{\frac{8}{9}(y-1)^2 - \frac{1}{2} + \frac{\xi^2}{2}y'^2}{2\bar{a}} - \Delta c_0\,\theta' y\right] + \frac{1}{2\tau^2}\theta^2 + \frac{1}{2}\theta'^2\right\}. \tag{21}$$

This gives rise to the two linear Euler-Lagrange equations

$$\begin{aligned}\frac{\xi^2}{2}y'' &= \frac{8}{9}(y-1) - \bar{a}\,\Delta c_0\,\theta',\\ \theta'' &= \frac{1}{\tau^2}\theta + \Delta c_0\,\phi_{eq}y',\end{aligned} \tag{22}$$

which need to be solved subject to the boundary conditions $y(x = 0) = 0$, $\theta'(x = 0) = 0$, $y(x \to \infty) = 1$, and $\theta(x \to \infty) = 0$. Inserting the Euler-Lagrange equations back into Eq. (21) and using the boundary conditions allows us to compute an expression for the excess free energy, namely, the line tension

$$\sigma = \frac{8}{3}\frac{\xi^2}{a}\phi_{eq}^4 y'(0) + \kappa\phi_{eq}\,\Delta c_0\,\theta(0). \tag{23}$$

Because the Euler-Lagrange Eqs. (22) are linear, it is straightforward to identify their analytic solution

$$\begin{aligned}y(x) &= 1 + \frac{e^{-\omega_1 x}\left[(\omega_2\tilde{\xi})^2 - 1\right] - e^{-\omega_2 x}\left[(\omega_1\tilde{\xi})^2 - 1\right]}{(\omega_1^2 - \omega_2^2)\tilde{\xi}^2},\\ \theta(x) &= \frac{\Delta c_0\,\phi_{eq}}{(\omega_1^2 - \omega_2^2)\tilde{\xi}^2}\left(\frac{e^{-\omega_1 x}}{\omega_1} - \frac{e^{-\omega_2 x}}{\omega_2}\right),\end{aligned} \tag{24}$$

where we have defined $\tilde{\xi} = 3\xi/4$. The two inverse characteristic lengths ω_1 and ω_2 satisfy the equations

$$\omega_1^2 + \omega_2^2 = \frac{1}{\tau^2} + \frac{1}{\tilde{\xi}^2}\left(1 - s^2\right), \qquad \omega_1\omega_2 = \frac{1}{\tau\,\tilde{\xi}}, \tag{25}$$

where we have introduced the quantity

$$s = \Delta c_0\sqrt{\frac{9}{8}\bar{a}\,\phi_{eq}} = \frac{3}{8}\frac{\Delta c_0}{\phi_{eq}}\sqrt{\frac{3}{2}a\kappa}. \tag{26}$$

It is useful to analyze how the two inverse characteristic lengths behave as function of s. For a sufficiently small magnitude $|s| < s^{tr}$, both ω_1 and ω_2 are positive real numbers, indicating a double-exponential decay of $y(x)$ and $\theta(x)$. In the region, $s^{tr} < |s| < s^{max}$, the two quantities $\omega_1 = \omega_r + i\omega_c$ and $\omega_2 = \omega_r - i\omega_c$ are conjugate complex numbers, implying that $y(x)$ and $\theta(x)$ exhibit spatially damped oscillations. The prediction of damped oscillations for the spatial relaxation of lipid layers and other amphiphilic systems is not uncommon,[39,40] especially when more than one order parameter is needed to describe their energetic behavior. For $|s| > s^{max}$, the monolayer is structurally unstable, with undamped oscillations due to both ω_1 and ω_2 being imaginary numbers. We find

$$s^{tr} = \left|1 - \frac{\tilde{\xi}}{\tau}\right|, \qquad s^{max} = 1 + \frac{\tilde{\xi}}{\tau}. \tag{27}$$

Two other special cases deserve to be mentioned. At $|s| = s^{bal}$, the real and imaginary parts ω_r and ω_c are equal to each other, $\omega_r = \omega_c$. Finally, at $|s| = s^{van}$ the line tension σ, which we calculate below [see Eq. (30)], vanishes. We find

$$s^{bal} = \sqrt{1 + \frac{\tilde{\xi}^2}{\tau^2}}, \qquad s^{van} = \sqrt{\left(1 + \frac{\tilde{\xi}}{\tau}\right)\frac{\tilde{\xi}}{\tau}}. \tag{28}$$

Note that the superscripts in Eqs. (27) and (28) stand for transition ("tr"), maximal ("max"), balanced ("bal"), and vanishing ("van"). If $\tilde{\xi} = \tau$, then $s^{tr} = 0$ and no regime of double-exponential decay exists; at the same time, $s^{bal} = s^{van}$ coincide.

In Fig. 3, we display the characteristic lengths based on the particular example $\xi = 2$ nm and $\tau = 1$ nm. This leads to $\tilde{\xi} = 1.5$ nm and thus $s^{tr} = 0.5$, $s^{bal} = 1.803$, $s^{van} = 1.936$, and $s^{max} = 2.5$. We show

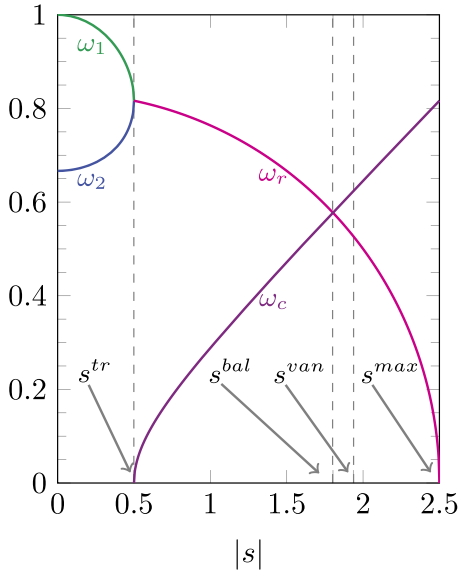

FIG. 3. Visualization of the solutions (in nm^{-1}) of Eq. (25) as function of $|s|$. For $0 < |s| < s^{tr}$, we display ω_1 (green) and ω_2 (blue), and for $s^{tr} < |s| < s^{max}$, we display ω_r (magenta) and ω_c (violet) with $\omega_1 = \omega_r + i\omega_c$ and $\omega_2 = \omega_r - i\omega_c$ being complex conjugate numbers. We also mark the values s^{bal} and s^{van}. The diagram is calculated for $\xi = 2$ nm and $\tau = 1$ nm, leading to $\tilde{\xi} = 1.5$ nm as well as to $s^{tr} = 0.5$, $s^{bal} = 1.803$, $s^{van} = 1.936$, and $s^{max} = 2.5$.

ω_1 (green) and ω_2 (blue) as a function of $|s|$ in the region $0 < |s| < s^{tr}$. We also show ω_r (magenta) and ω_c (violet) as a function of $|s|$ in the region $s^{tr} < |s| < s^{max}$. Note that Fig. 3 describes the principal physical behavior of the solutions $y(x)$ and $\theta(x)$ in the entire range of s, where the lipid monolayer has two stable coexisting bulk phases. If a, κ, and ϕ_{eq} are independent of Δc_0, then s is proportional to Δc_0, leading to the same behavior of the solutions when these are analyzed with respect to Δc_0. On the other hand, if a, κ, and ϕ_{eq} depend on Δc_0, then the function $s = s(\Delta c_0)$ is no longer necessarily linear in Δc_0.

To determine the line tension σ, we only need the two quantities $y'(0)$ and $\theta(0)$ [see Eq. (23)]. From Eq. (24), we obtain

$$y'(0) = \frac{1}{\bar{\xi}^2}\,\frac{1+\frac{\bar{\xi}}{\tau}}{\omega_1+\omega_2}, \qquad \theta(0) = -\frac{\tau}{\bar{\xi}}\,\frac{\Delta c_0\,\phi_{eq}}{\omega_1+\omega_2}, \tag{29}$$

which after insertion into Eq. (23) yields our final result for the approximate line tension

$$\sigma = \frac{8}{3}\,\frac{16}{9}\,\frac{\phi_{eq}^4}{a}\left(1+\frac{\bar{\xi}}{\tau}-s^2\,\frac{\tau}{\bar{\xi}}\right)\frac{1}{\omega_1+\omega_2}, \tag{30}$$

with s being specified in Eq. (26). Below, we demonstrate that Eq. (30) is an excellent approximation of the line tension in Eq. (13); it therefore constitutes the major result of the present work.

Clearly, if $\Delta c_0 = 0$, then $s = 0$ together with Eq. (25) implies $\omega_1 = 1/\bar{\xi}$ and $\omega_2 = 1/\tau$, yielding $\sigma = (32/9)\,\xi\,\phi_{eq}^4/a$, which is identical to Eq. (15). We also verify that $\sigma = 0$ in Eq. (30) gives rise to s^{van} as specified in Eq. (28).

B. Definition of reference state

Following Eq. (8), we have argued that the line tension σ depends only on the difference between the two spontaneous curvatures $\Delta c_0 = c_0^A - c_0^B$ but not on $\bar{c}_0 = (c_0^A + c_0^B)/2$. The quantity Δc_0 will serve as a control parameter in our work. Changing Δc_0 can be achieved by utilizing different types of lipids. Yet, this implies that, in general, all material parameters that appear in Eq. (1)—including a, χ, K, κ and κ_t—may be functions of Δc_0. Incorporating all possible dependencies into our model introduces at least five (in the case of linear relationships) additional parameters, of which none are known from experiments. This suggests us to focus instead on a small number of special cases that allow for a clear interpretation of the predictions of our model. To this end, we assume that only $\chi = \chi(\Delta c_0)$ may depend on Δc_0, whereas a, K, κ, and κ_t remain unaffected. Even more, we focus on only two cases for the function $\chi = \chi(\Delta c_0)$. In the first case, χ will not depend on Δc_0, and in the second case, χ will depend on Δc_0 in such a way that the compositions of the two bulk phases remain unaltered. In the following, we define the two cases accurately.

We first discuss our reference state, $\Delta c_0 = 0$. In this case, we introduce the notation $\chi(\Delta c_0 = 0) = \chi_0$, $\phi_{eq}(\Delta c_0 = 0) = \phi_0$, $\xi(\Delta c_0 = 0) = \xi_0$, and $\sigma(\Delta c_0 = 0) = \sigma_0$. Recall from Eqs. (4) and (5) that for $\Delta c_0 = 0$, we have $\chi_c = 2$ and thus $\Delta\chi = \chi_0 - 2$. Therefore, $\phi_0 = [(3/8)(\chi_0 - 2)]^{1/2}$, $\xi_0 = [K/(\chi_0 - 2)]^{1/2}$, and $\sigma_0 = (32/9)\xi_0\phi_0^4/a$ or, equivalently,

$$K = \sqrt{2a\sigma_0\xi_0^3}, \qquad \chi_0 = 2 + \sqrt{\frac{2a\sigma_0}{\xi_0}}, \qquad \phi_0 = \left(\frac{9}{32}\,\frac{a\sigma_0}{\xi_0}\right)^{1/4}. \tag{31}$$

If reasonable values for a, ξ_0, and σ_0 can be estimated or extracted from experiment, we can determine K, χ_0, and ϕ_0 through Eq. (31).

As mentioned above, we will focus only on two scenarios for the dependence of χ on the difference between the spontaneous curvatures c_0^A and c_0^B. We specify these two cases as

$$\chi = \chi_0 + \epsilon\,\frac{a}{2}\kappa\,(\Delta c_0)^2, \tag{32}$$

with ϵ adopting one of two values, either $\epsilon = 0$ or $\epsilon = 1$. Because of $\Delta\chi = \chi_0 - 2 + (\epsilon - 1)(a/2)\,\kappa\,(\Delta c_0)^2$, we can specify how ϕ_{eq} and ξ depend on Δc_0. From Eqs. (8), (9), and (31), we find

$$\phi_{eq} = \sqrt{\frac{3}{8}\left[\sqrt{\frac{2a\sigma_0}{\xi_0}} + (\epsilon-1)\,\frac{a}{2}\kappa\,(\Delta c_0)^2\right]}, \qquad \xi = \frac{\xi_0}{\sqrt{1+(\epsilon-1)\frac{a}{2}\kappa\,(\Delta c_0)^2\sqrt{\frac{\xi_0}{2a\sigma_0}}}}. \tag{33}$$

This also yields the Δc_0-dependencies of $\bar{\xi} = 3\xi/4$, of s in Eq. (26), and of ω_1 and ω_2 in Eq. (25), thus fully specifying the Δc_0-dependence of the line tension $\sigma = \sigma(\Delta c_0)$.

We note that for $\epsilon = 0$, an increase in $|\Delta c_0|$ moves the coexisting compositions $\pm\,\phi_{eq}$ closer to each other until, for

$$\Delta c_0^{lim} = \left(\frac{8\,\sigma_0}{a\,\kappa^2\,\xi_0}\right)^{1/4}, \tag{34}$$

the compositional difference between the bulk phases vanishes, $\phi_{eq} = 0$. Then, there is no phase transition anymore, implying that the line tension σ vanishes. We expect (and demonstrate below) that in this case the reduction of σ with growing $|\Delta c_0|$ mainly reflects the diminishing mismatch between the two bulk phases. We refer to the case $\epsilon = 0$ as that of *adjusting bulk phases*.

For the other case, $\epsilon = 1$, we find $\phi_{eq} = \phi_0$ and $\xi = \xi_0$. Hence, the change in Δc_0 does not alter the bulk phase compositions $\pm\phi_{eq}$. This case is the most interesting one because the change in line tension σ with growing $|\Delta c_0|$ reflects exclusively the restructuring of the interfacial region without being affected by an additional adjustment of the bulk phases. We refer to the case $\epsilon = 1$ as that of *non-adjusting bulk phases*.

In this work, we choose for our reference state $a = 0.65$ nm^2, $\sigma_0 = 0.1\ k_BT$/nm, $\kappa = 10\ k_BT$, $\kappa_t = 10\ k_BT$/nm^2, and $\xi_0 = 2$ nm. The cross-sectional area per lipid a and bending stiffness κ correspond to typical values in lipid layers.[41] The magnitude of the tilt modulus agrees with recent theoretical estimates[32,34] and coarse-grained computer simulations.[42] Experimental[1–3,6,13,17] and computational[43] observations of the line tension in lipid monolayers and bilayers exhibit significant variations but are generally on the order of 1 pN, thus motivating our choice for σ_0. Computational studies also suggest ξ_0 to be on the nm-range.[43] Inserting our selected reference

values into Eq. (31) yields $\pm\phi_0$ with $\phi_0 = 0.31$ for the compositions of the two coexisting bulk phases.

C. Comparison of numerical results and analytic approximation

We are now ready to compare numerical solutions of the full non-linear model [Eqs. (11) and (13)] with the approximate analytic results [Eqs. (24) and (30)]. We also provide an interpretation of our findings.

1. Adjusting bulk phases

We first consider the case $\epsilon = 0$, where a change in Δc_0 leaves all other material parameters unaffected. Figure 4 shows $y(x) = \phi(x)/\phi_{eq}$ [panel (a)] and $\theta(x)$ [panel (b)] for three different values of $\Delta c_0 < 0$. Note that switching the sign of Δc_0 merely changes the sign of $\theta(x)$ thereby leaving $y(x)$ and σ unaffected. The inset of Fig. 4 shows the maximum tilt angle $\theta^{max} = \theta(0)$ as function of Δc_0. Recall that for the analytic approximation, the maximum tilt angle is specified in Eq. (29), with ϕ_{eq}, $\tilde{\xi}$, ω_1, and ω_2 all being functions of Δc_0. It appears that our approximation in Eq. (18) reproduces the functions $y(x)$ and $\theta(x)$—including the maximum θ^{max}—with high accuracy. A maximum in $|\theta^{max}|$ as a function of $|\Delta c_0|$ appears because the matching of a growing spontaneous curvature difference by a growing non-vanishing tilt angle $|\theta^{max}|$ is counteracted by the decrease in ϕ_{eq}. Indeed, according to Eq. (33), we find the decreasing equilibrium bulk compositions $\phi_{eq} = 0.304$ for $\Delta c_0 = -0.05$/nm, $\phi_{eq} = 0.216$ for $\Delta c_0 = -0.2$/nm, and $\phi_{eq} = 0.139$ for $\Delta c_0 = -0.25$/nm, which cause θ^{max} to eventually decrease. Ultimately, at $|\Delta c_0| = \Delta c_0^{lim} = 0.28$/nm, the bulk phases become identical, $\phi_{eq} = 0$, implying the absence of a phase transition and $\theta^{max} = 0$.

The profiles of $y(x)$ and $\theta(x)$ in Fig. 4 appear not to involve spatially decaying oscillations. That is, ω_1 and ω_2 are both real-valued. Let us analyze under what conditions we will observe oscillations.

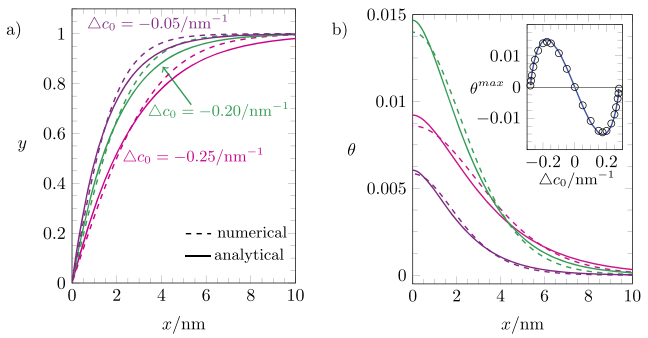

FIG. 4. (a) Compositional profile $y(x) = \phi(x)/\phi_{eq}$ and (b) tilt angle $\theta(x)$ measured in radians, for the case of adjusting bulk phases ($\epsilon = 0$), with $\Delta c_0 = -0.05$/nm (violet), $\Delta c_0 = -0.20$/nm (green), and $\Delta c_0 = -0.25$/nm (magenta). The inset in (b) shows $\theta^{max} = \theta(0)$ as a function of Δc_0. Dashed lines (and open circles in the inset) correspond to numerical results of the non-linear model according to Eq. (11); solid lines display the analytic approximation according to Eq. (24). In all calculations, we have used $a = 0.65$ nm^2, $\kappa = 10\ k_BT$, $\kappa_t = 10\ k_BT$/nm^2, $\xi_0 = 2$ nm, and $\sigma_0 = 0.1\ k_BT$/nm. The equilibrium bulk compositions are $\phi_{eq} = 0.304$ for $\Delta c_0 = -0.05$/nm, $\phi_{eq} = 0.216$ for $\Delta c_0 = -0.2$/nm, and $\phi_{eq} = 0.139$ for $\Delta c_0 = -0.25$/nm.

To this end, we consider the condition $s^{tr} = |1 - \tilde{\xi}/\tau|$ that separates the double-exponential decay from the regime of spatially decaying oscillations [see Eq. (27)]. With the definitions of s [Eq. (26)] and the expressions for ϕ_{eq} and ξ [Eq. (33) for $\epsilon = 0$], we rewrite the condition for s^{tr} as

$$\tilde{s}^{tr}(\tilde{s}) = \left|\sqrt{1 - \frac{8}{9}\tilde{s}^2} - \frac{3}{4}\frac{\xi_0}{\tau}\right|, \tag{35}$$

expressed in terms of the variable

$$\tilde{s} = \frac{3}{8}\frac{\Delta c_0}{\phi_0}\sqrt{\frac{3}{2}a\kappa}. \tag{36}$$

Note that $\tilde{s}$ becomes identical to s in Eq. (26) if ϕ_0 is replaced by ϕ_{eq}. Hence, $\tilde{s}/(\Delta c_0) = [s/(\Delta c_0)]_{\Delta c_0 \to 0}$. Transitioning between the double-exponential and damped oscillating regimes requires the equation $\tilde{s}^{tr}(\tilde{s}) = \tilde{s}$ to be fulfilled. To identify the critical value of the ratio ξ_0/τ where the transition starts to occur, we solve that equation together with the additional equation $d\tilde{s}^{tr}/d\tilde{s} = 1$, leading to $\xi_0/\tau = \sqrt{34}/3 = 1.94$ and $\tilde{s} = 9/(2\sqrt{34}) = 0.77$. Hence, for $\xi_0/\tau > 1.94$, we will always observe double-exponential behavior, whereas for ξ_0/τ slightly smaller than 1.94, there is a re-entrant behavior as function of growing $|\Delta c_0|$: from double-exponential decay to damped oscillations and then back to double-exponential decay. The re-entrant behavior starts for $\xi_0/\tau = 1.94$ at $\Delta c_0 = 0.217$/nm. Because Fig. 4 corresponds to $\xi_0/\tau = 2$, only double-exponential decay is observed.

Figure 5 shows the line tension σ as function of $|\Delta c_0|$ (see the solid blue line, which applies to $\epsilon = 0$). We have marked the point $\Delta c_0^{lim} = 0.28$/nm at which $\phi_{eq} = 0$ and phase separation ceases to occur. Clearly, the line tension σ decays fast from its reference value $\sigma_0 = 0.1\ k_BT$/nm to $\sigma = 0$ because of the assistance from the

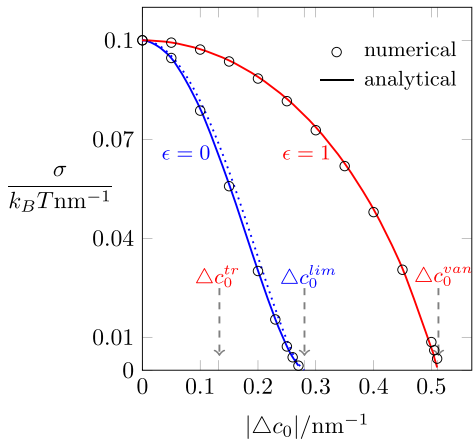

FIG. 5. Line tension $\sigma(\Delta c_0)$ for $\epsilon = 0$ (blue) and $\epsilon = 1$ (red). Open circles correspond to numerical result of the non-linear model according to Eqs. (11) and (13); solid lines display the analytic approximation according to Eq. (30). The blue dotted line shows the line tension obtained when we only account for the indirect Δc_0-dependence of σ in Eq. (15) through ϕ_{eq} and ξ given by Eq. (33). In all calculations, we have used $a = 0.65$ nm^2, $\kappa = 10\ k_BT$, $\kappa_t = 10\ k_BT$/nm^2, $\xi_0 = 2$ nm, and $\sigma_0 = 0.1\ k_BT$/nm. For the case $\epsilon = 0$ this leads to $\Delta c_0^{lim} = 0.28$/nm. For the case $\epsilon = 1$, this leads to $\Delta c_0^{tr} = 0.132$/nm and $\Delta c_0^{van} = 0.511$/nm.

Δc_0-induced decrease of ϕ_{eq}. The assistance is in fact an almost complete dominance. To demonstrate this, we have included into Fig. 5 the curve given by Eq. (15) (the dotted blue line) that is obtained by enforcing $\theta(x) = 0$. This neglects the direct Δc_0-dependence of σ and, instead, accounts only for the indirect Δc_0-dependence through ϕ_{eq} and ξ, as specified in Eq. (33). The indirect Δc_0-dependence of σ arises exclusively from adjustments of the two coexisting bulk phases, for which the lipid tilt degree of freedom is irrelevant. Clearly, dotted and solid blue lines in Fig. 5 almost coincide, thus demonstrating the dominance of the indirect over the direct dependence of σ on Δc_0. Hence, when calculating the line tension between two coexisting phases as a function of a control parameter (such as the difference in spontaneous curvatures Δc_0), it is important to not neglect the influence of that parameter on the bulk phases. Specifically, in case our control parameter Δc_0 only affects the spontaneous curvature $c_0(\phi) = \bar{c}_0 + \Delta c_0\, \phi$ of the lipid layer but no other quantity, the line tension is determined largely by the influence of the spontaneous curvature on the bulk phases, not by the influence of the spontaneous curvature on the interfacial structure.

2. Non-adjusting bulk phases

For the case $\epsilon = 1$, the interaction parameter χ in Eq. (32) adjusts so as to fix $\phi_{eq} = \phi_0$, leaving also $\xi = \xi_0$ unaffected [see Eq. (33)]. Growing $|\Delta c_0|$ then leads exclusively to changes in the interfacial structure, without affecting the bulk phases. Figure 6 displays the compositional profile $y(x)$ and tilt angle $\theta(x)$ for different choices of $\Delta c_0 < 0$ [here again, changing the sign of Δc_0 changes only the sign of $\theta(x)$]. The inset of Fig. 6 shows the maximum tilt angle $\theta^{max} = \theta(0)$ as function of Δc_0. In contrast to Fig. 4, some of the profiles exhibit spatially decaying oscillations. From s^{tr} in Eq. (27) and the definition of s in Eq. (26), we find that $|\Delta c_0| = \Delta c_0^{tr}$ with

$$\Delta c_0^{tr} = \frac{8}{3}\phi_0 \sqrt{\frac{2}{3a\kappa}} \left|1 - \frac{3}{4}\frac{\xi_0}{\tau}\right| = 0.132\ \mathrm{nm}^{-1} \tag{37}$$

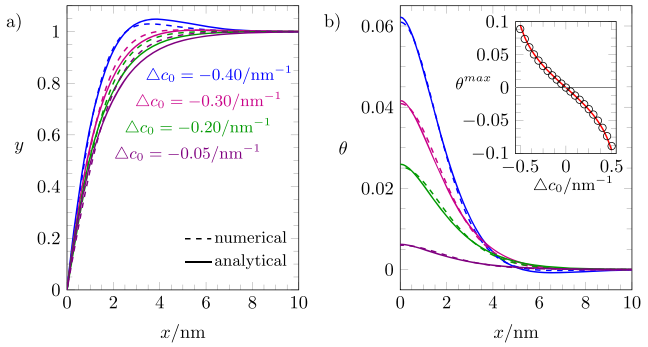

FIG. 6. (a) Compositional profile $y(x) = \phi(x)/\phi_{eq}$ and (b) tilt angle $\theta(x)$ measured in radians, for the case of non-adjusting bulk phases ($\epsilon = 1$), with $\Delta c_0 = -0.05$/nm (violet), $\Delta c_0 = -0.2$/nm (green), $\Delta c_0 = -0.3$/nm (magenta), and $\Delta c_0 = -0.4$/nm (blue). The inset in (b) shows $\theta^{max} = \theta(0)$ as a function of Δc_0. Dashed lines (and open circles in the inset) correspond to numerical results of the non-linear model according to Eq. (11); solid lines display the analytic approximation according to Eq. (24). In all calculations, we have used $a = 0.65$ nm^2, $\kappa = 10\ k_BT$, $\kappa_t = 10\ k_BT$/nm^2, $\xi_0 = 2$ nm, and $\sigma_0 = 0.1\ k_BT$/nm. This leads to $\Delta c_0^{tr} = 0.132$/nm, $\Delta c_0^{bal} = 0.476$/nm, $\Delta c_0^{van} = 0.511$/nm, and $\Delta c_0^{max} = 0.660$/nm.

separating the regimes of double-exponential decay from spatially decaying oscillations. Further on, at $|\Delta c_0| = \Delta c_0^{bal} = 0.476$/nm, the real and imaginary parts ω_r and ω_c of $\omega_1 = \omega_r + i\omega_c$ and $\omega_2 = \omega_r - i\omega_c$ are equal to each other. Next, at $|\Delta c_0| = \Delta c_0^{van} = 0.511$/nm, the line tension σ vanishes, as can indeed be observed in Fig. 5 (the red line corresponds to $\epsilon = 1$). We note that despite the vanishing line tension, the bulk phases remain stable. Only for $|\Delta c_0| > \Delta c_0^{max} = 0.660$/nm do the bulk phases develop a structural instability. As already observed in Fig. 4, our analytic approximation given by Eq. (24) (solid lines in Fig. 6) is an excellent approximation of the numerical solution to the full non-linear Euler-Lagrange equations given by Eq. (11) (broken lines in Fig. 6 and open circles in the inset of Fig. 6). For the line tension, the agreement becomes virtually quantitative—compare the solid lines in Fig. 5 [the approximate analytic result according to Eq. (30)] to the open circles [the numerical result of the full non-linear problem according to Eq. (13)]. When the effective lipid-lipid interaction parameter $\chi = \chi(\Delta c_0)$ depends on our control parameter Δc_0 such that the bulk phase compositions $\phi_{eq} = \phi_0$ remain strictly constant, then the line tension σ decays slowly as function of growing $|\Delta c_0|$. Eventually, however, it decreases to zero, and it does so before the bulk phases develop a structural instability. Despite $\phi_{eq} = \phi_0$ remaining constant, the line tension decreases as a function of $|\Delta c_0|$ because the monolayer is able to employ the interfacial region to alleviate some of the frustration energy that is stored in the bulk phases.

IV. CONCLUSIONS

The standard Landau-Ginzburg model for the interfacial profile and line tension between two coexisting fluid phases is based on one single order parameter—the density for a compressible single-component fluid or the composition for an incompressible binary fluid.[30] For a binary lipid monolayer, the tilt angle $\theta = \theta(x)$ of the lipid tails suggests to introduce a second order parameter, in addition to the scaled composition $y(x)$. In this work, we have analyzed the ensuing two order parameter Landau-Ginzburg model and its prediction for the interfacial profile, $y(x)$ and $\theta(x)$, and line tension σ between two coexisting phases in a lipid monolayer. Employing a previously introduced double-parabola approximation[24,37,38] into the free energy functional linearizes the Euler-Lagrange equations and leads to simple, and yet remarkably accurate, analytic expressions for $y(x)$, $\theta(x)$, and σ. The approximation also allows us to identify two different physical regimes: a double-exponential decay and spatially decaying oscillations of the interfacial profile.

Our model describes binary fluid-like lipid monolayers at the air-water interface that phase separate as function of their composition at fixed lateral pressure. This is reminiscent of mixed lipid bilayers that phase separate into domains. However, lipid bilayers are characterized by yet another order parameter, the bilayer thickness. Despite some attempts to include tilt and thickness into calculations of elastic membrane properties,[44] no three-order parameter Landau-Ginzburg model (including tilt, thickness, and composition) for a binary lipid bilayer has been proposed and analyzed so far. Including membrane thickness into the present model is thus a possible extension. For lipid monolayers at the air-water interface, the monolayer

thickness does not entail an energetically relevant hydrophobic mismatch between domains (yet, it can contribute to the miscibility[45]) and is thus ignored in the present work. We have also neglected changes of the local cross-sectional area per molecule a, assuming instead that a is fixed and constant in both coexisting phases. This approximation prevents us from having to account for different dipole densities of different domains. Including changes in a would appear as yet another order parameter in a Landau-Ginzburg model.

The model proposed in this work was motivated by recent experimental findings from Bischof *et al.*[2] where an increase of the line tension in binary lipid monolayers was observed as a function of spontaneous curvature. Our present work, although suggesting a decrease of σ as a function of Δc_0 in Fig. 5, is not necessarily in disagreement with the experimental findings. Recall that, in general, all material parameters, especially χ and K, can depend on the spontaneous curvature. In our model, we have only investigated the two physically most interesting cases, where either only Δc_0 is changed or where χ changes with Δc_0 so that the bulk phases remain unaffected. A general relationship between χ and Δc_0 (and similarly between K and Δc_0) can easily be selected such that σ increases with Δc_0. However, little is known about these relationships, so we have not included them into our present model.

ACKNOWLEDGMENTS

This work resulted from a visit of E.R.F. at the Physics Department of North Dakota State University, supported through Fulbright Commission and CONICET (Consejo Nacional de Investigaciones Científicas y Técnicas, Argentina). R.D. and S.M. thank the Phospholipid Research Center in Heidelberg, Germany, for support.

APPENDIX: FREE ENERGY CALCULATION

We derive Eq. (12) using Eq. (10), Eq. (11), and the boundary conditions. Equation (10) can be expressed equivalently as

$$\frac{\tilde{F}}{L} = \kappa \int_{-\infty}^{\infty} dx \left\{ \phi_{eq} \frac{-y\left(y - \frac{1}{2}y^3 + \frac{\xi^2}{2}y''\right) + \frac{\xi^2}{2}\left(y'y\right)'}{2\bar{a}} - \phi_{eq}\Delta c_0\, \theta' y - \frac{1}{2}\theta\left(-\frac{\theta}{\tau^2} + \theta''\right) + \frac{1}{2}\left(\theta'\theta\right)' \right\}. \tag{A1}$$

Based on the Euler-Lagrange equations, we can replace $y - y^3/2 + \xi^2 y''/2$ by $y^3/2 - \bar{a}\,\Delta c_0\,\theta'$ and $-\theta/\tau^2 + \theta''$ by $\Delta c_0\,\phi_{eq} y'$. We also note that the two terms $(y'y)'$ and $(\theta'\theta)'$ in the integrand can be integrated and, owing to the boundary conditions $y'(\pm\infty) = \theta'(\pm\infty) = 0$, do not contribute to the free energy $\tilde{F}/L$. This leaves us with the expression

$$\frac{\tilde{F}}{L} = \kappa \int_{-\infty}^{\infty} dx \left\{ \frac{\phi_{eq}}{2\bar{a}}\left(-\frac{1}{2}y^4 + \bar{a}\,\Delta c_0\,\theta' y\right) - \Delta c_0\,\phi_{eq}\theta' y - \frac{1}{2}\Delta c_0\,\phi_{eq}\left[(\theta y)' - \theta' y\right] \right\}. \tag{A2}$$

Here again, the term $(\theta y)'$ can be integrated and contributes nothing to $\tilde{F}/L$ because of the boundary condition $\theta(\pm\infty) = 0$. All other terms that are proportional to Δc_0 cancel out. The resulting expression is Eq. (12).

REFERENCES

[1] I. Sriram and D. K. Schwartz, "Line tension between coexisting phases in monolayers and bilayers of amphiphilic molecules," Surf. Sci. Rep. **67**, 143–159 (2012).
[2] A. A. Bischof and N. Wilke, "Molecular determinants for the line tension of coexisting liquid phases in monolayers," Chem. Phys. Lipids **165**, 737–744 (2012).
[3] N. Wilke, "Lipid monolayers at the air–water interface: A tool for understanding electrostatic interactions and rheology in biomembranes," in *Advances in Planar Lipid Bilayers and Liposomes* (Elsevier, 2014), Vol. 20, pp. 51–81.
[4] J. P. Hagen and H. M. McConnell, "Liquid-liquid immiscibility in lipid monolayers," Biochim. Biophys. Acta, Biomembr. **1329**, 7–11 (1997).
[5] P. Krüger, M. Schalke, Z. Wang, R. H. Notter, R. A. Dluhy, and M. Lösche, "Effect of hydrophobic surfactant peptides SP-B and SP-C on binary phospholipid monolayers. I. Fluorescence and dark-field microscopy," Biophys. J. **77**, 903–914 (1999).
[6] H. M. McConnell, "Structures and transitions in lipid monolayers at the air-water interface," Annu. Rev. Phys. Chem. **42**, 171–195 (1991).
[7] A. Tian, C. Johnson, W. Wang, and T. Baumgart, "Line tension at fluid membrane domain boundaries measured by micropipette aspiration," Phys. Rev. Lett. **98**, 208102 (2007).
[8] C. D. Blanchette, W.-C. Lin, C. A. Orme, T. V. Ratto, and M. L. Longo, "Using nucleation rates to determine the interfacial line tension of symmetric and asymmetric lipid bilayer domains," Langmuir **23**, 5875–5877 (2007).
[9] A. J. García-Sáez, S. Chiantia, and P. Schwille, "Effect of line tension on the lateral organization of lipid membranes," J. Biol. Chem. **282**, 33537–33544 (2007).
[10] D. Lingwood and K. Simons, "Lipid rafts as a membrane-organizing principle," Science **327**, 46–50 (2010).
[11] A. R. Honerkamp-Smith, P. Cicuta, M. D. Collins, S. L. Veatch, M. den Nijs, M. Schick, and S. L. Keller, "Line tensions, correlation lengths, and critical exponents in lipid membranes near critical points," Biophys. J. **95**, 236–246 (2008).
[12] B. L. Stottrup, J. TigreLazo, V. B. Bagonza, J. C. Kunz, and J. A. Zasadzinski, "Comparison of line tension measurement methods for lipid monolayers at liquid–liquid coexistence," Langmuir **35**, 16053 (2019).
[13] D. J. Benvegnu and H. M. McConnell, "Line tension between liquid domains in lipid monolayers," J. Phys. Chem. **96**, 6820–6824 (1992).
[14] C. Esposito, A. Tian, S. Melamed, C. Johnson, S.-Y. Tee, and T. Baumgart, "Flicker spectroscopy of thermal lipid bilayer domain boundary fluctuations," Biophys. J. **93**, 3169–3181 (2007).
[15] B. L. Stottrup, A. M. Heussler, and T. A. Bibelnieks, "Determination of line tension in lipid monolayers by Fourier analysis of capillary waves," J. Phys. Chem. B **111**, 11091–11094 (2007).
[16] M. C. Heinrich, I. Levental, H. Gelman, P. A. Janmey, and T. Baumgart, "Critical exponents for line tension and dipole density difference from lipid monolayer domain boundary fluctuations," J. Phys. Chem. B **112**, 8063–8068 (2008).
[17] D. W. Lee, Y. Min, P. Dhar, A. Ramachandran, J. N. Israelachvili, and J. A. Zasadzinski, "Relating domain size distribution to line tension and molecular dipole density in model cytoplasmic myelin lipid monolayers," Proc. Natl. Acad. Sci. U. S. A. **108**, 9425–9430 (2011).
[18] W. T. Góźdź and G. Gompper, "Composition-driven shape transformations of membranes of complex topology," Phys. Rev. Lett. **80**, 4213 (1998).
[19] P. S. Kumar, G. Gompper, and R. Lipowsky, "Budding dynamics of multicomponent membranes," Phys. Re. Lett. **86**, 3911 (2001).
[20] D. Andelman, T. Kawakatsu, and K. Kawasaki, "Equilibrium shape of two-component unilamellar membranes and vesicles," Europhys. Lett. **19**, 57 (1992).
[21] T. Kawakatsu, D. Andelman, K. Kawasaki, and T. Taniguchi, "Phase transitions and shapes of two component membranes and vesicles I: Strong segregation limit," J. Phys. II **3**, 971–997 (1993).
[22] T. Taniguchi, K. Kawasaki, D. Andelman, and T. Kawakatsu, "Phase transitions and shapes of two component membranes and vesicles II: Weak segregation limit," J. Phys. II **4**, 1333–1362 (1994).

[23]G. Gompper and S. Zschocke, "Elastic properties of interfaces in a Ginzburg-Landau theory of swollen micelles, droplet crystals and lamellar phases," Europhys. Lett. **16**, 731 (1991).
[24]G. Gompper and S. Zschocke, "Ginzburg-Landau theory of oil-water-surfactant mixtures," Phys. Rev. A **46**, 4836 (1992).
[25]T. Taniguchi, "Shape deformation and phase separation dynamics of two-component vesicles," Phys. Rev. Lett. **76**, 4444 (1996).
[26]H. Y. Chan and V. Lubchenko, "Pressure in the Landau-Ginzburg functional: Pascal's law, nucleation in fluid mixtures, a meanfield theory of amphiphilic action, and interface wetting in glassy liquids," J. Chem. Phys. **143**, 124502 (2015).
[27]P. Hohenberg and A. Krekhov, "An introduction to the Ginzburg–Landau theory of phase transitions and nonequilibrium patterns," Phys. Rep. **572**, 1–42 (2015).
[28]P. Fonda, M. Rinaldin, D. J. Kraft, and L. Giomi, "Thermodynamic equilibrium of binary mixtures on curved surfaces," Phys. Rev. E **100**, 032604 (2019).
[29]H. T. Davis, *Statistical Mechanics of Phases, Interfaces, and Thin Films* (VCH, New York, 1996).
[30]N. Provatas and K. Elder, *Phase-Field Methods in Materials Science and Engineering* (John Wiley & Sons, 2011).
[31]S. Safran, *Statistical Thermodynamics of Surfaces, Interfaces, and Membranes* (CRC Press, 2018).
[32]S. May, Y. Kozlovsky, A. Ben-Shaul, and M. Kozlov, "Tilt modulus of a lipid monolayer," Eur. Phys. J. E **14**, 299–308 (2004).
[33]M. Hamm and M. Kozlov, "Tilt model of inverted amphiphilic mesophases," Eur. Phys. J. B **6**, 519–528 (1998).
[34]M. Hamm and M. Kozlov, "Elastic energy of tilt and bending of fluid membranes," Eur. Phys. J. E **3**, 323–335 (2000).
[35]S. May, "Protein-induced bilayer deformations: The lipid tilt degree of freedom," Eur. Biophys. J. **29**, 17–28 (2000).
[36]To formally show this, consider the Euler-Lagrange equations first subject to the boundary conditions $y(x_0) = 0$, $\theta'(x_0) = 0$, $y(x_0 + L) = 1$, $\theta(x_0 + L) = 0$, where x_0 and L are arbitrary, with $L > x_0$. Symmetry of the Euler-Lagrange equations implies that the solution $y(x_0 + x)$ and $\theta(x_0 + x)$ in the region $x_0 \le x \le x_0 + L$ can be used to construct another solution $-y(x_0 - x)$ and $\theta(x_0 - x)$, which satisfies the boundary conditions $y(x_0 - L) = -1$, $\theta(x_0 - L) = 0$, $y(x_0) = 0$, $\theta'(x_0) = 0$. That is, the functions $y(x_0 + x)$ and $\theta(x_0 + x)$, which are odd and even with respect to x_0, solve the Euler-Lagrange equations subject to the boundary conditions $y(x_0 - L) = -1$, $\theta(x_0 - L) = 0$, $y(x_0 + L) = 1$, $\theta(x_0 + L) = 0$. This argument holds for any L. When L grows to infinity, the position x_0 still exists. In our work, we identify that position with the origin of the coordinate system, $x_0 = 0$, which corresponds to the boundary conditions $\lim_{L\to\infty} y(x = \pm L) = \pm 1$ and $\lim_{L\to\infty} \theta(x = \pm L) = 0$.
[37]R. Lipowsky, "Long-range correlations at depinning transitions. I," Z. Phys. B: Condens. Matter **55**, 335–343 (1984).
[38]A. J. Jin and M. E. Fisher, "Effective interface Hamiltonians for short-range critical wetting," Phys. Rev. B **47**, 7365 (1993).
[39]G. Gompper and M. Schick, "Correlation between structural and interfacial properties of amphiphilic systems," Phys. Rev. Lett. **65**, 1116 (1990).
[40]N. Dan, P. Pincus, and S. Safran, "Membrane-induced interactions between inclusions," Langmuir **9**, 2768–2771 (1993).
[41]D. Marsh, "Elastic curvature constants of lipid monolayers and bilayers," Chem. Phys. Lipids **144**, 146–159 (2006).
[42]X. Wang and M. Deserno, "Determining the lipid tilt modulus by simulating membrane buckles," J. Phys. Chem. B **120**, 6061–6073 (2016).
[43]S. Baoukina, E. Mendez-Villuendas, and D. P. Tieleman, "Molecular view of phase coexistence in lipid monolayers," J. Am. Chem. Soc. **134**, 17543–17553 (2012).
[44]P. I. Kuzmin, S. A. Akimov, Y. A. Chizmadzhev, J. Zimmerberg, and F. S. Cohen, "Line tension and interaction energies of membrane rafts calculated from lipid splay and tilt," Biophys. J. **88**, 1120–1133 (2005).
[45]F. Dupuy and B. Maggio, "The hydrophobic mismatch determines the miscibility of ceramides in lipid monolayers," Chem. Phys. Lipids **165**, 615–629 (2012).